SIMULATED MIGRATION AMPLITUDES: THEORY AND APPLICATIONS

T. Kaschwich and H. Bolin

email: *tina@norsar.no*

keywords: *Modeling, PSDM, Converted waves, Anisotropy*

ABSTRACT

Illumination maps are a useful tool for survey planning and for QC of amplitudes picked on selected target horizons. The Simulated Migration Amplitude technique (SMA) is a ray-based un-weighted Kirchhoff migration of synthetic data around seismic reflectors. In order to enhance illumination mapping for hydrocarbon exploration and reservoir imaging in complex subsurface structures, we present the extension of the SMA to converted waves and in anisotropic media. We demonstrate the accuracy of this method for a synthetic 2.5D example. The calculated amplitudes for both PP and PS waves are compared to real pre-stack depth migration amplitudes. For this example, the SMA results are equal to results from pre-stack depth migration. Finally, we document the influence of different model and wave types on illumination studies.

INTRODUCTION

Exploration geophysicists have historically relied on seismic PP-reflection experiments together with the assumption of an isotropic subsurface. Thus seismic experiments are cheap, the fundamental theory is simple, and processing techniques are fast. However, today's exploration areas are often more complex, the targeted reservoirs are increasingly smaller and at deeper positions, e.g. for targets beneath salt bodies and basalt layers. Furthermore, shale's, which make up 75% of the sedimentary cover of the hydrocarbon reservoirs, are mostly anisotropic. Also converted waves are used more often to image reservoirs and to improve reservoir characterization. To meet these requirements, a greater effort in survey planning, seismic acquisition and data processing is necessary. Especially, survey planning is important in order to optimize the seismic acquisition in terms of cost/benefit. Therefore, it has become common practice to model a hypothetical reflection data set in order to plan the acquisition geometry (i.e. source and receiver locations) to receive an optimum image of the subsurface (e.g. Sassolas et al., 1999; Muerdter and Ratcliff, 2001). To study the illumination of a particular target horizon in depth, usually 3D forward ray tracing of reflected rays is coupled with target-oriented binning methods.

Since conventional illumination mapping, i.e. counting hits or adding amplitudes in bin cells, neither takes the Fresnel volume nor the seismic pulse into account, the calculated maps approximate only crudely the results of pre-stack depth migration (PSDM) (see Laurain and Vinje, 2001).

To improve the obtained amplitudes, Schneider and Winbow (1999) described a direct simulation of a depth migration. Later, Laurain et al. (2002) introduced a technique for PP reflections, called Simulated Migration Amplitude (SMA), which is a Kirchhoff migration of ray synthetic data around known seismic reflectors. Their method uses an approximation of the true travel time field around reflection points to generate amplitude maps. Both, the source pulse and the Fresnel zone, are taken into account in this approach.

After a brief introduction of the general SMA concept we show a synthetic case study for computing amplitude maps by a readapted SMA computation to consider effects like anisotropy and attenuation in the subsurface model and noise on illumination studies.

METHOLOGY

Illumination studies are a usefull tool for survey planing before acquisition or controlling and understanding of amplitude distributions after migration. Assuming, for instance, the SEG salt model (see Figure 1a) the computed hit map (Figure 1c) indicates that a large area below the salt will not be illuminated. This effect is also visible in the corresponding SMA map (Figure 1d). In order to compute these maps first all needed quantities are calculated by wavefront construction and dynamic ray tracing (Figure 1b). The resulting illumination maps are generated for a zero-offset survey (701 shots with a shot distance of 20m). However, applying this approach for various survey configurations could lead to better subsalt illumination and thus the actual acquisition geometry can be optimized.

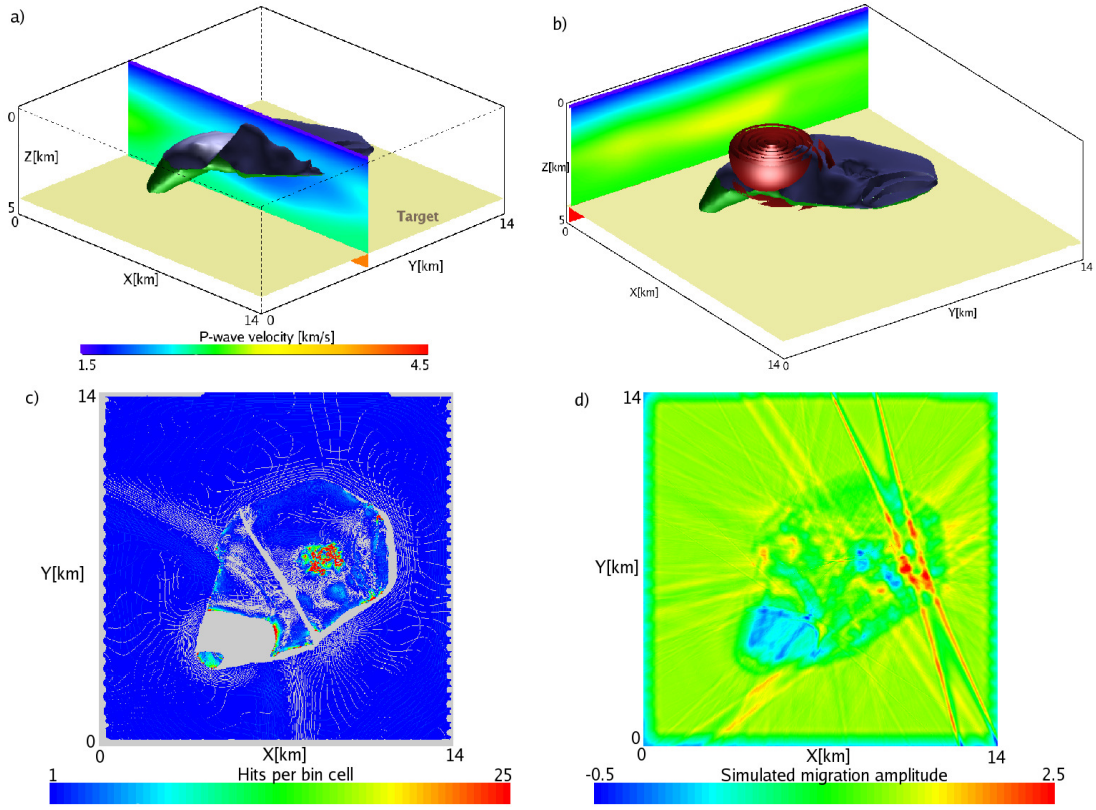

Figure 1: (a) SEG salt model; the SMA uses information gained by wavefront construction including dynamic ray tracing (b) to compute afterwards the hit map (c) and the corresponding SMA map (d).

As SMA maps are a simulation of PSDM amplitudes, we are going to present the similarities between a real migration and the simulation process. According to Bleistein and Gray (2001) the mathematical expression for the Kirchhoff migration can be written as:

$$\beta^{PSDM}(x) = \int W(x,\xi)\mathcal{F}[U(\xi, t = \tau(x,\xi))]d\xi \tag{1}$$

where x indicates a depth point, U are seismic traces, $\mathcal{F}$ is a filter function needed to correctly recover the shape of the source pulse, ξ are the trace locations, the travel time from shot to receiver via x is denoted by $\tau(x,\xi)$, $W(x,\xi)$ is the migration weight function, and $\beta^{PSDM}(x)$ is the migration amplitude at the depth point x.
During the migration procedure the two-way travel time function $\tau(x,\xi)$ for each source-receiver pair is computed in a background velocity model. This is usually done by either ray tracing or Eikonal solvers

and requires a significant amount of CPU time and disk space. Figure 2 shows the basic concept of the SMA method. As for conventional amplitude maps, this approach requires a velocity model, either layered or smooth, and, thus, a good knowledge of the target reflector(s), in order to model the reflected rays.

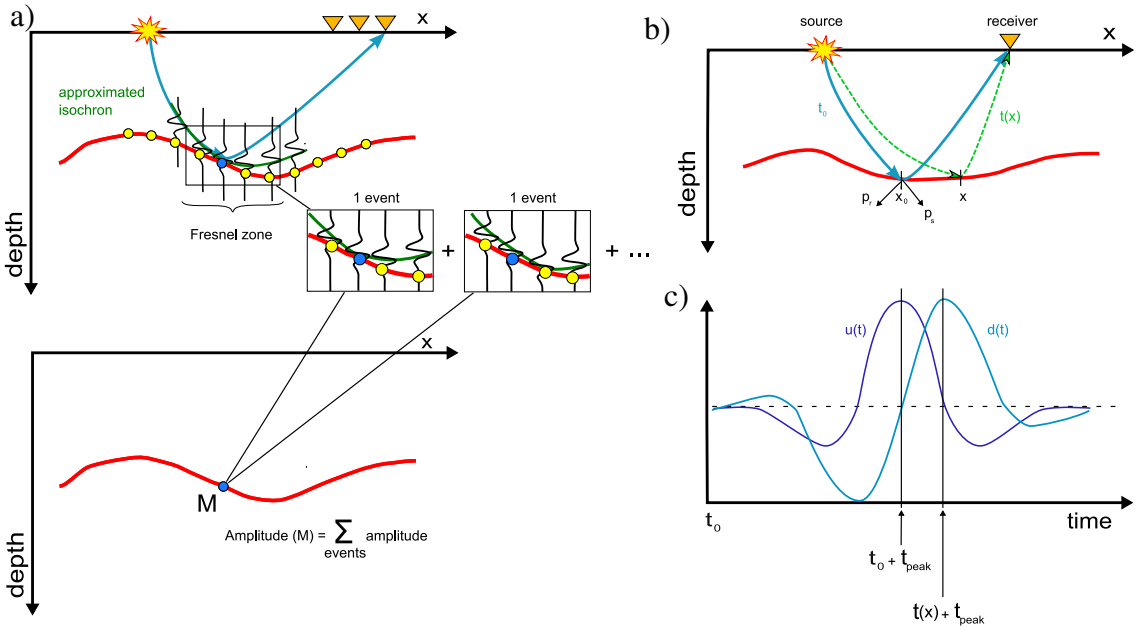

Figure 2: SMA concept: (a) Stacking of the pulse along the target reflector, where the pulse touches the reflector, each seismic trace is replaced by a corresponding synthetic trace and the summation over all image points leads to amplitude in image point M; (b) the two-way second-order traveltime approximation is used; the input trace is filtered ($d(t) = F[u(t)]$) depending on the dimensionality (c).

The main differences between conventional un-weighted migration and the SMA that lead to a significant improvement of the overall CPU time are that:

- each seismic trace $U(\xi, t)$ is replaced by a corresponding synthetic trace generated by ray tracing,
- the exact two-way traveltimes are substituted by two-way traveltimes estimated by a second-order paraxial approximation,
- stacking of the pulse is done only along the target in the area, where the pulse touches the reflector.

Like for migration the summation over all events leads to the final amplitude in image point M (see Figure 2a). Compared to equation (1) the corresponding mathematical expression for the SMA can be described by

$$\beta^{SMA}(x) = \int W(x,\xi)\mathcal{F}[u(\xi, t = \tau_R(x,\xi))]d\xi. \tag{2}$$

The two-way travel time (see Figure 2b) in point x near reflection point x_0 is computed by paraxial approximation (Červený et al., 1984):

$$\tau_R(x,\xi) = \tau_s(x_0) + \tau_r(x_0) + (p_s(x_0) + p_r(x_0))^T \Delta x + +\frac{1}{2}\Delta x^T(\hat{M}_s(x_0) + \hat{M}_r(x_0))\Delta x, \tag{3}$$

where $\tau_s(x_0)$ is the travel time of the down-going wave to point x_0 and $\tau_r(x_0)$ the travel time for up-going wave reflected in x_0, and Δx is given by $(x - x_0)$. The approximation includes the two slowness vectors in x_0, $p_s(x_0)$ and $p_r(x_0)$ (source and receiver sides, respectively), and the 3×3 matrices of second-order derivatives of one-way travel times in x_0, $\hat{M}_s(x_0)$ and $\hat{M}_r(x_0)$. All quantities on the right hand side are

calculated by dynamic ray tracing using the Wavefront Construction method (Vinje et al., 1996) which is be performed in a previous model step (see Gjøystdal et al., 2007). However, all quantities can also be obtained for converted waves (PS conversion) or in the presence of anisotropy in the velocity model. Computation and accuracy considerations on this time approximation are described by Mispel et al. (2003). Using the arrival time of the specular ray, the corresponding synthetic input trace $u(t)$ is constructed from the real source pulse by adding their Hilbert transform as an imaginary part:

$$\begin{aligned} u(t) &= Re(A_0)s(t-t_0) - Im(A_0)h(t-t_0), \quad t \in [t_0, t_0+T] \\ u(t) &= 0, \qquad\qquad\qquad\qquad\qquad\quad t \ni [t_0, t_0+T] \end{aligned} \tag{4}$$

where $s(t)$ is the causal source pulse with duration T and its Hilbert transform $h(t)$. The complex amplitude A_0 is estimated by ray tracing. The applied filter function $\mathcal{F}$ depends on the dimensionality of the problem (Bleistein and Gray, 2001). Based on the fact that this approach uses ray tracing the SMA allows multi-arrivals.

COMPARISON TO PSDM RESULTS

We apply the SMA method to a target reflector separating two layers of constant velocities, see Figure 3a. The velocity values are 2250 and 2750m/s above and below the reflector, respectively, but the density is constant in the entire model. A common shot survey is specified, with 120 shots located between 2 and 8 km in the inline direction (shot spacing 50 m). The source pulse is a zero-phase Ricker wavelet with a central frequency of 20 Hz. Source-receiver offsets have ranges between 0 and 1 km, and the receiver spacing is 25 m. Two synthetic seismic data sets (PP and PS reflections) were generated using ray tracing.

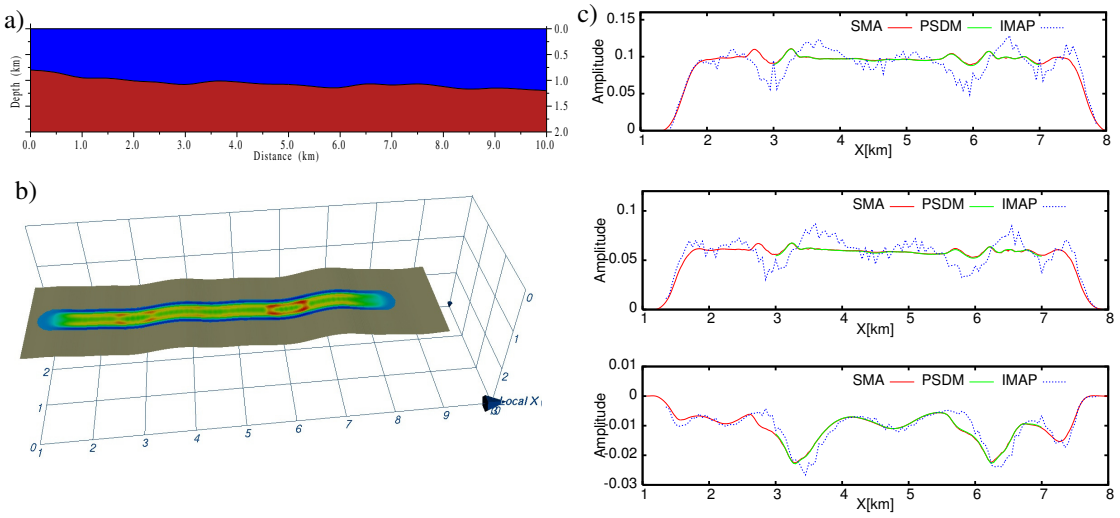

Figure 3: Comparison of SMA maps with PSDM results: (a) Synthetic model; (b) SMA distributed for a PP reflection on the target reflector (map generated for a 20-Hz Ricker wavelet); (c) Picked amplitudes for PP-reflections (top), x-component (middle) and z-component of the PS-reflection.

Kaschwich and Mispel (2006) introduced the SMA for converted waves. These data sets were subsequently depth migrated, and migration amplitudes were extracted along the reflector. Thereafter, the same survey and model setup was used to simulate migration amplitudes on the target reflector. The results for each wave type are shown in Figure 3c. In both cases the SMA and PSDM amplitude profiles match almost exact. There are small differences due to the different travel time approximation, which are used in both approaches. For comparison, the results for the conventional illumination amplitude (IMAP) are also shown, which have much stronger variations.

INFLUENCE OF DIFFERENT MODEL AND WAVE-TYPE

A good survey planing is needed to deliver the best-possible imaging quality necessary to better explore and exploit the many complex, often unconventional reservoirs, e.g., tight sands and fractured shales, commonly targeted by industry today. Using all available subsurface information in the design of a 3-D seismic survey could help to adjust the acquisition effort to demands of illuminating the target horizon. In this regards converted seismic waves e.g. for targets beneath salt bodies and basalt layers, are of increasing interest for the exploration of subsurface targets. To meet these demands the SMA process computes hit and amplitude maps for both pressure (P) and shear (S) wave reflections and by comparing corresponding attributes for both wave modes (PP- and PS- reflections), their capability to illuminate a target structure can be predicted or limitations of either wave mode can be revealed.
In this section we are using a simplified reservoir model, see Figure 4a, to compute amplitude maps for either PP or PS reflections and increasing the complexity of the model by introducing an anisotropic shale layer and considering attenuation for P- waves within the reservoir.

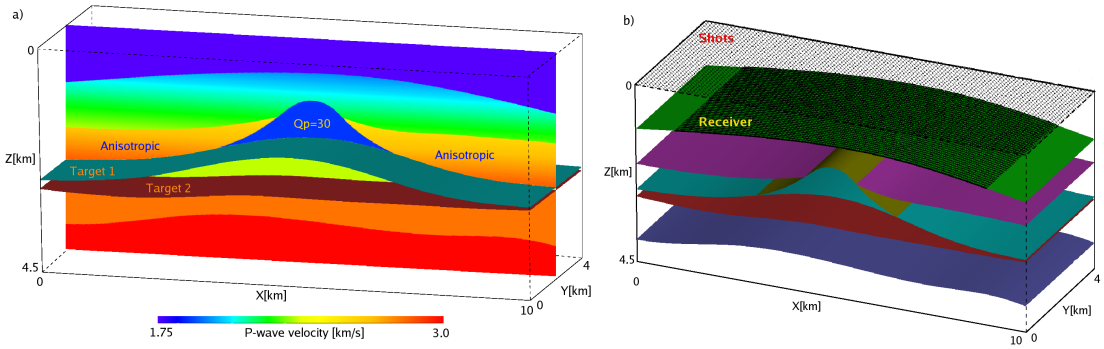

Figure 4: Synthetic test model for different wave and model types (a); OBS survey with 2121 shots and 16441 receivers fixed at the sea bed (b).

To simulate a real converted wave acquisition, we computed all following amplitude maps for an OBS survey (see Figure 4b). Shots were modeled over the entire model with a shot spacing of 100 m inline and 200 m crossline. The receivers are fixed at the seabed between 1 and 9 km inline (20m spacing) and crossline between 0 and 4 km with a 100 m receiver-line spacing. The source pulse is a zero-phase Ricker wavelet with a central frequency of 20Hz. The S-wave velocities are defined by a constant P/S ratio of 1.732 (see Figure 5a) and the density is given in Figure 5b.

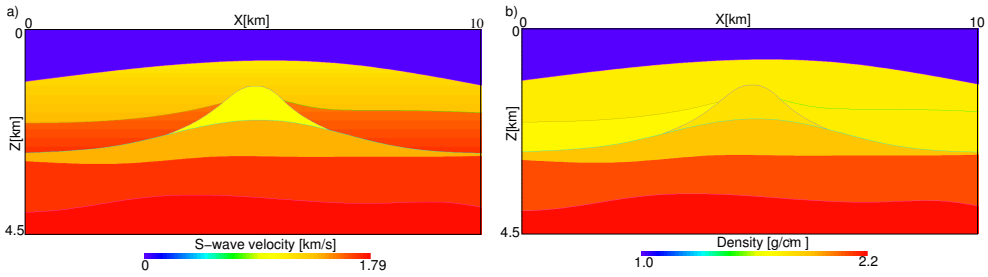

Figure 5: S-wave velocities (a) and density (b) for the synthetic salt model.

For this first calculation the model is assumed to be isotropic, and after running the wavefront tracer the illumination maps for both wave modes are calculated (see Figure 6). Here, the conventional imaging workflow for converted waves is performed, i.e., first derive the radial component data from the two horizontal

components and then do the single component (or scalar) imaging process using the radial component. The radial component signal is the projection of inline and crossline signal on the radial direction (pointing from source to receiver) and is a mixture of S_v and S_H waves. In particular, if the subsurface is anisotropic and the two shear waves have different propagation velocities, the image from the prestack depth migration and consequently the SMA profile, will be degraded because of the mixture of the two waves. However, the scalar migration is an established imaging tool and thus the radial component is used for the generation of the SMA maps for the converted waves.

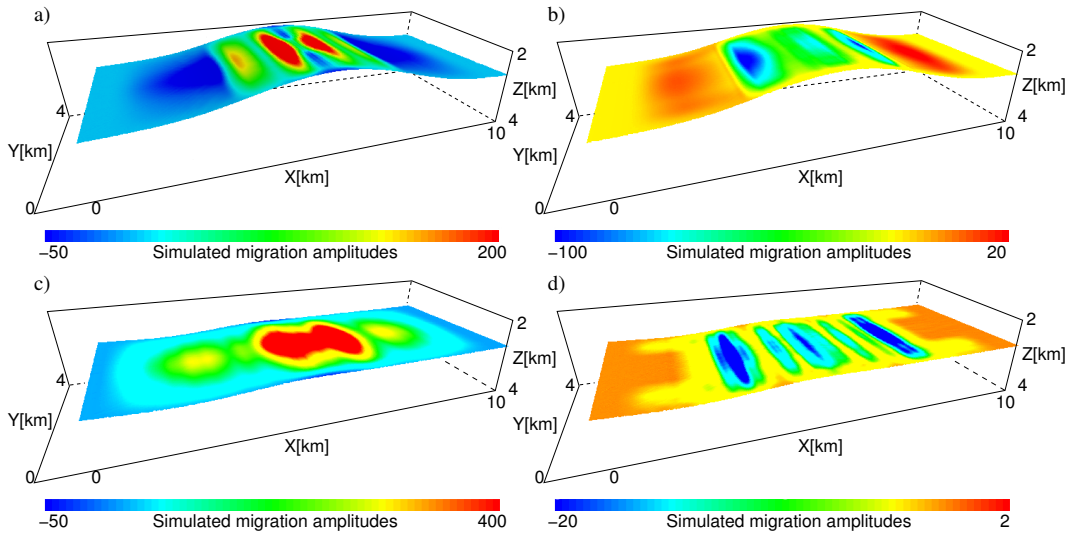

Figure 6: SMA for both wave modes: computed for PP-reflections for the upper (a) and lower (c) target reflector; and the radial component of the PS-reflection for the upper (b) and lower (d) target reflector.

Under the consideration that the attenuation within the reservoir does not differ from the surrounding sediments the PP reflections have larger illumination amplitudes for both target reflectors. However, the illuminated area appears to be larger for converted waves, and the distribution of the amplitude maxima and minima differs noticeably from the PP reflection amplitudes. Depending on a P-wave attenuation in the reservoir the converted waves could give a better positioning of the reservoir boundaries.

Anisotropy

Shales comprise a large proportion of most sedimentary basins and form the seal and source rocks for many hydrocarbon reservoirs. Often shale formations are anisotropic and therefore, anisotropy is becoming an important issue in exploration and reservoir geophysics. The origin of seismic anisotropy in shales is non-unique and may be attributed to several factors, e.g. including preferred orientation of clay platelets, microcracks, fine-layering and/or stress-induced anisotropy. However, incorporating anisotropy into imaging algorithms will facilitate the correct positioning of the reservoir targets.
To demonstrate the potential of the SMA to support better acquisition planing in the presence of anisotropy, we introduce an anisotropic shale layer with tiled symmetry axis. The anisotropy is given by the Thomsen parameters $\epsilon = 0.2$ and $\delta = -0.1$. Furthermore, we consider that the anisotropic shale layer was deformed after deposition and therefore the axis of symmetry is normal to the bedding (see Figure 7).

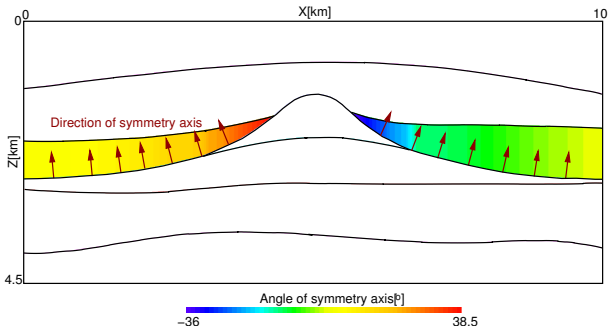

Figure 7: Angles of the axis of symmetry for the titled anisotropic shale layer.

The resulting amplitude maps are displayed in Figure 8. In addition an amplitude difference plot between the isotropic and anisotropic model is shown for both target reflectors. Here, the red color indicated regions where the amplitude for the anisotropic model was larger and blue areas with higher isotropic illumination amplitudes, respectively. This simple example already illustrates the significant influence on illumination studies ignoring anisotropic effects.

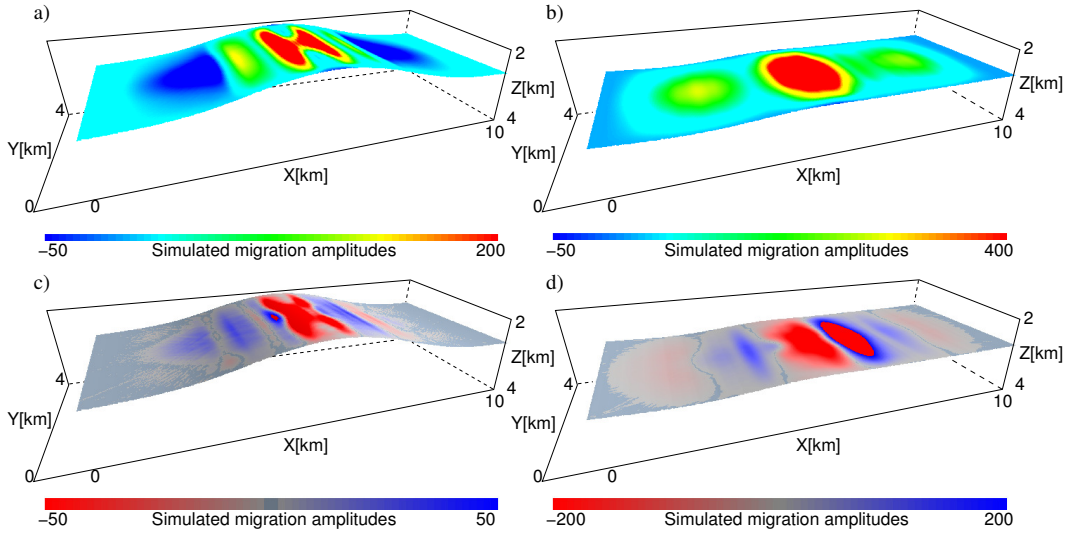

Figure 8: SMA maps for PP with anisotropic shale layer for the upper (a) and the lower (b) target reflector; difference plot for each horizon between amplitudes for the isotropic and the anisotropic subsurface model.

Attenuation

A seismic wave looses energy as it propagates through the earth. A subsurface reservoir full of hydrocarbons tends to be acoustically softer than if it is full of an incompressible fluid such as water. Theoretical models of seismic wave attenuation predict that a wave passing through such a reservoir should suffer more attenuation than in surrounding materials. It is proposed that this anomalously high attenuation can be detected in seismic data and used as an indicator for the presence of a hydrocarbon reservoir. The ability of a rock to attenuate seismic waves is usually measured by a dimensionless quantity called Q. A lossless material has a Q of infinity while a completely lossy material has a Q of zero. Rocks are found to have Q values in the range 10-400 with the typical sedimentary rock having a value near 100. The SMA implementation was modified so that the seismic attenuation for P waves can be considered (see Figure 9). However, within the SMA computation we replaced the wavelet by the non-causal attenuated one.

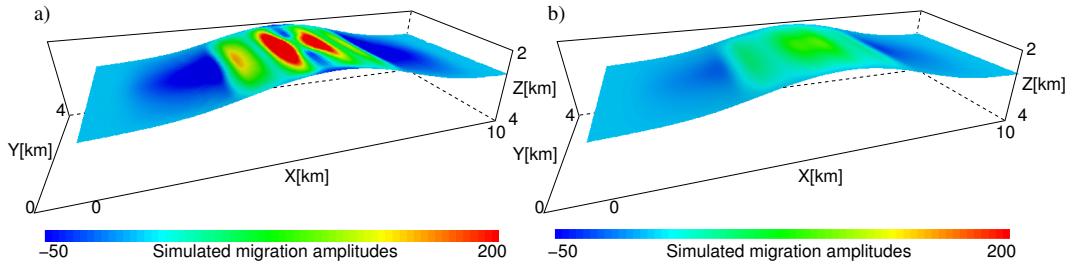

Figure 9: SMA maps for PP reflections without (a) and with attenuation (b) computed for the upper target horizon.

For this example, a relative high value for Q of 30 is assumed and the chosen target reflector lies just below the reservoir as labeled in Figure 4 by target 1. Without considering attenuation the area of the reflector located below the reservoir appears to be illuminated (see Figure 9a). However, when considering attenuation, the same area shows almost no illumination amplitudes (see Figure 9b).

Noise

Real pre-processed seismic sections contain always residual noise that affects the amplitudes after migration. Consequently, including noise in the SMA method will improve the comparability with real PSDM results and will thus help with the interpretation of the SMA maps.
Unlike PSDM, SMA considers only one reflector, limits the size of the trace to the pulse length and limits the migration operator to the Fresnel zone. The effect of noise could be simulated in two ways: 1) by adding noise on the synthetic data before SMA or 2) by adding "post-migration" noise on the calculated SMA map. We have studied the first possibility by including band-limited Gaussian noise to the synthetic data before summation. However, even if the effect of noise can be seen qualitatively in the SMA maps, a detailed analysis showed that amplitudes and spatial frequencies of the SMA results differ significantly from the PSDM results. Therefore, the SMA implementation allows to include noise by setting a specific threshold or by adding an imported noise grid to the SMA map. Figure 10 shows SMA maps for the two different target horizons where imported noise was added, respectively. The here considered random noise could be replaced by any kind of noise distribution observed, measured or assumed after a real migration process.

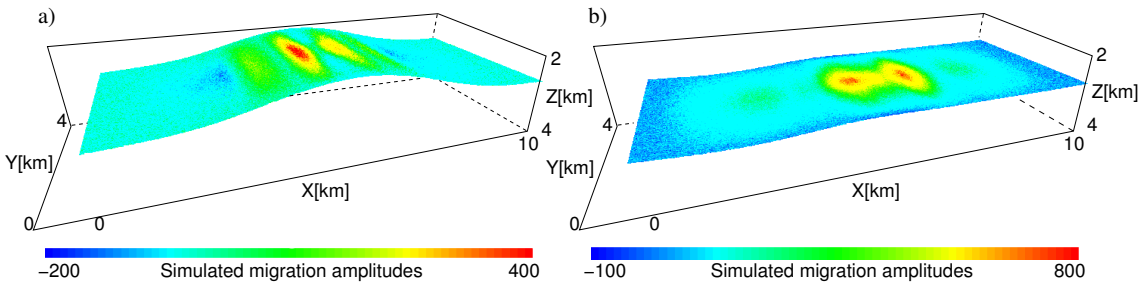

Figure 10: SMA maps with different noise level for (a) target horizon 1 the lower border of the reservoir and target horizon 2.

CONCLUSIONS

Illumination studies are important for cost/benefit analyses during the survey planning process. Because of the increasing relevance of converted waves, we extended the Simulated Migration Amplitude (SMA)

method, proposed by Laurain et al. (2002) for PP waves, to PS waves. The comparison with PSDM amplitudes in controlled synthetic models show a strong similarity to the real PSDM amplitude maps, whereas conventional illumination amplitude maps seems to exaggerate the amplitude variations on the reflector. Furthermore, SMA is considerably faster than PSDM, since it does not need to access the pre-stack data and only a small portion of the synthetic time trace is stacked within a (Fresnel) zone in the vicinity of the reflection point.
Accurately mapping subsurface salt flank and sub-salt structures are critical tasks for exploration and reservoir characterization. The given synthetic example demonstrates the differences in the illumination for PP and PS waves. Furthermore, we were able to show that considering anisotropy for this synthetic saltmodel results in larger illumination amplitude below the reservoir. These results make us confident that the SMA analysis extended to converted waves and anisotropic media can significantly improve future survey planning in the presents of complex subsurface structures. In addition, the SMA approach can consider noise and attenuation effects to obtain more reliable and realistic amplitudes.

ACKNOWLEDGMENTS

We thank the Research Council of Norway, project 181688/I30 (Imaging) and NORSAR and NORSAR Innovation for permission to publish the results.

REFERENCES

Bleistein, N. and Gray, S. (2001). From the hagedoorn imaging technique to kirchhoff migration and inversion. *Geophys. Prosp.*, 49:629–643.

Červený, V., Klimes, L., and Pšenčik, I. (1984). Paraxial ray approximation in the computation of seismic wavefields in inhomogeneous media. *Geophys. J.R. astr. Soc.*, pages 89–104.

Gjøystdal, H., Iversen, E., Lecomte, I., Kaschwich, T., Drottning, Å., and Mispel, J. (2007). Improved applicability of ray tracing in seismic acquisition, imaging and interpretation. *Geophysics*, 72:SM261–SM271.

Kaschwich, T. and Mispel, J. (2006). Simulated migration amplitudes of converted waves: First results. *76st Ann. Internat. Mtg., Soc. of Expl. Geophys.*, pages 2574–2578.

Laurain, R., Mispel, J., and Vinje, V. (2002). Toward better amplitude maps by simulated migration. *72st Ann. Internat. Mtg., Soc. of Expl. Geophys.*

Laurain, R. and Vinje, V. (2001). Prestack depth migration and illumination maps. *71st Ann. Internat. Mtg., Soc. of Expl. Geophys.*, pages 929–932.

Mispel, J., Iversen, E., Vinje, V., Laurain, R., and Lecomte, I. (2003). Local two-way traveltime approximations in 3d media. *65th Mtg.: Eur. Assn. of Expl. Geophys.*

Muerdter, D. and Ratcliff, D. (2001). Understanding subsalt illumination through ray-tracing modeling, part 1: Simple 2-d salt models. *The Leading Edge*, 20(6):578–595.

Sassolas, C., Lescoffit, G., and Nicodeme, P. (1999). The benefits of 3-d ray tracing in acuistion feasibility. *Annual Meeting Abstracts, Soc. of Expl. Geophys.*, pages 633–632.

Schneider, W. J. and Winbow, G. (1999). Efficient and accurate modeling of 3-d seismic illumination. *69st Ann. Internat. Mtg., Soc. of Expl. Geophys.*, pages 633–636.

Vinje, V., Iversen, E., Åstebøl, K., and Gjøystdal, H. (1996). Estimation of multivalued arrivals in 3D models using wavefront construction- Part I&II. *Geophys. Prosp.*, 44:819–858.